



HAL
open science

A comparative study of natural Tunisian clay types in the formulation of compacted earth blocks

S. Mkaouar, W. Maherzi, P. Pizette, H. Zaitan, M. Benzina

► To cite this version:

S. Mkaouar, W. Maherzi, P. Pizette, H. Zaitan, M. Benzina. A comparative study of natural Tunisian clay types in the formulation of compacted earth blocks. *Journal of African Earth Sciences*, 2019, 160, 10.1016/j.jafrearsci.2019.103620 . hal-03225113

HAL Id: hal-03225113

<https://hal.science/hal-03225113>

Submitted on 21 Dec 2021

HAL is a multi-disciplinary open access archive for the deposit and dissemination of scientific research documents, whether they are published or not. The documents may come from teaching and research institutions in France or abroad, or from public or private research centers.

L'archive ouverte pluridisciplinaire **HAL**, est destinée au dépôt et à la diffusion de documents scientifiques de niveau recherche, publiés ou non, émanant des établissements d'enseignement et de recherche français ou étrangers, des laboratoires publics ou privés.



Distributed under a Creative Commons Attribution - NonCommercial 4.0 International License

1 A comparative study of natural Tunisian clay types in the formulation of compacted earth
2 blocks

3

4

5 Safa MKAOUAR ^{1,2*}, Walid MAHERZI ², Patrick PIZETTE ², Hicham ZAITAN ³ and
6 Mourad BENZINA¹

7

8 ¹Laboratory "Water, Energy and Environment" (LR3E), National Engineering School of Sfax, University of Sfax, Tunisia.

9 ²IMT Lille Douai, Univ. Lille, EA 4515 - LGCgE - F-59000 Lille, France.

10 ³Laboratory "Chemistry of Condensed Matter" (LMCC), Faculty of Science and Technology Fez, University of Sidi
11 Mohammed Ben Abdellah, Morocco.

12 *Corresponding author

13 E-mail address: safa_mkaouar@yahoo.com

14 **Abstract**

15 This study investigates the physico-chemical, mineralogical and thermal characteristics of
16 three natural Tunisian clays collected from Gafsa (A1), Zeramdine (A2) and Nabeul (A3).
17 The aim was to promote an appropriate formulation of materials and to obtain optimal
18 compacted earth blocks (CEB). Results of mineralogical analysis of clays revealed the
19 dominance of kaolinite (> 13.58%), illite (>25.7%), quartz (> 18%) and a minor fraction of
20 smectite phases. Chemical analysis of the clays major elements showed a SiO₂ content
21 exceeding 50% and a percentage of Al₂O₃ higher than 18%. Particle size distribution showed
22 that clay fractions varied from 10 to 20 %. Plasticity index defined a plastic character while
23 the values of specific surface area were around 60 m²/g. This discrepancy has an effect on the
24 behavior of these clays in CEB, notably their mechanical properties. From this
25 characterization, it appears that all the sampled clays are suitable as raw material for CEB
26 application. The prepared CEB formulations varied according to compaction energy and
27 binder dosages. In this work, lime served as a binder at different rates (4, 6, 8 and 10%) to
28 ameliorate the quality of CEB. Unconfined Compressive Strength values were determined by
29 Static method test. Then bulk density, shrinkage and porosity values of samples were

1 determined. Compressive strength could reach 7 MPa with lime supplementation in sample
2 A1. The static compaction onto the sand-clay mixture achieved a value of density superior to
3 2 g.cm^{-3} with lime supplementation in sample A1. Overall, the Gafsa clay was the most
4 suitable for CEB preparation. Also, lime improved the compressive strength of the matrix, in
5 addition to its ecological merits.

6

7 **Key words**

8 Clay, physico-chemical characterization, compressed earth blocks, lime, packing density,
9 compressive strength.

10

11 **Highlights**

12 * Tunisian clays from Nabeul, Zeramdine and Gafsa were investigated

13 * An ecofriendly and optimal CEB formulation was sought.

14 * Mixtures preparation influences physical and mechanical properties of CEB

15 * Lime use as a binder improves mechanical properties of CEB.

16 *Correlation could be established between porosity, shrinkage, packing density and strength
17 of the CEB.

18

19

20

21

22

23

24

25

26

27

1 **1. Introduction**

2 The production process of fired clay bricks has a considerable negative impact on the
3 environment [1]. This implies significant production costs, due to fuel prices and huge CO₂
4 emissions in the nature that contribute to increased greenhouse effects which leads to global
5 warming [2]. Therefore, the need to produce low-cost and eco-friendly construction materials
6 has become a major concern [3, 4]. Developing new sustainable building materials is a prime
7 consideration in the preservation of the environment [4, 3]. In fact, the harmful impact of
8 building materials on the environment must be reduced throughout their life cycle. New
9 technologies based on optimizing the choice of raw materials play an important role in this
10 approach by using ecological, local and renewable materials. In particular, earth is considered
11 the oldest source of building materials with low acquisition cost. A more ecological
12 alternative to the common fired clay brick is the compressed earth block (CEB) [1].
13 Interestingly, this building material has attracted much interest and several attempts to
14 optimize its formulation have been made. Morton indicated that CEB could win more than
15 80% of energy compared with fired clay brick [5].

16 Tunisia is endowed with an abundance and diversity of geological clay minerals. In this
17 context, some Tunisian clays were the objective of this study. Materials from three Tunisian
18 sites were characterized and tested for CEB formulation at different clay/sand proportions.
19 Also, lime was used as a binder and the mechanical strength of the different matrices were
20 compared.

21 **2. Materials: Geological setting**

22 Three different clay samples were used in this study. The first sample was collected from
23 Djebel Bouamrane "Gafsa" located in Southwest of Tunisia. This clay is red and belongs to
24 the Turonian age and Beida formation. The second clay was obtained from Zeramdine quarry
25 (Jemmel) "Monastir" in the Northeast of Tunisia. It is a white clay of Serravallien-Totonian
26 age and Oum Douil formation. The third one was brought from Djebel Abderrahmane
27 "Nabeul" (situated in Northeast of the country). This type of clay is green, of Serravalian age
28 and Souaf formation. Samples were tagged A1, A2 and A3, respectively as represented in Fig.
29 1. At first sight, it appears clearly that the main difference between these three types of clays
30 is due to their origin. The composition and structure of clays depends on their origin as well
31 as geology of the location.

32

1 After extraction, each sample was grinded and dried in an oven at 60°C until a constant
2 weight was reached.

3 In this present study, clay deposits were identified and characterized in terms of their
4 physicochemical, mineralogical and morphological properties.

5 **3. Methods**

6 **3.1. Materials identification and characterization**

7 Samples were characterized by several chemico-physical methods, which allowed us to
8 classify and compare clay characteristics and behaviors. Grain size analysis determines the
9 particle distribution of samples and allows to classify the materials according to their
10 Constituent parts (clay, sand, gravel). This test was performed to standard 13 320-1 and using
11 Coulter LS 13 320 Laser device and Fraunhofer 780d optical model. The detection particles
12 size was range from 0.375 μm to 2 mm.

13 Casagrande method describes the samples plastic behavior by the determination of Atterberg
14 Limits. Liquid limit (LL), plastic limit (PL) and plasticity index (PI) were determined
15 according to standard [NF P 94-051 \(1993\)](#) and [GTR-LCPC \(1987\)](#) [7, 8]. Specific gravity G_s
16 of solid grains was determined using an AccuPyc 1330 helium gas pycnometer.

17 Chemical composition of the clay was determined using Bruker S4 based on X-Ray
18 Fluorescence spectrometry measurements. Loss on ignition consists on placing samples in a
19 furnace with temperature of 550°C for 3 hours to determine its mass loss. Volatile substances
20 lost consist of molecular water carbon dioxide from carbonates and the presence of organic
21 matter.

$$22 \quad \text{Percent LOI} = ((\text{wet weight} - \text{dry weight}) / \text{dry weight}) * 100$$

23 Mineralogical composition of the clay samples was determined by X-Ray-Diffraction using
24 an Advance Bruker AXS D8 energy dispersion diffractometer to determine the mineral phases
25 in the material. This method concerns analyzing raw powder clay and randomly oriented
26 preparation: air-dried (at room temperature), saturated with ethylene glycol (EG) and heated
27 to 550°C for 1 h of the clay fraction after centrifugation. The preparation of oriented blades
28 was performed according to [Moore and Reynolds, 1997](#) [9].

29 Specific Surface Area and pores volume of samples were obtained by azote adsorption
30 isotherms methods at -196°C using a Micromeritics BET ASAP 2010 sorptometer.
31 Morphological features of the clays were analyzed by a Scanning Electron Microscope
32 Hitachi S-3600N apparatus.

1 Thermo-Gravimetric-Analysis (TGA) was performed by a Netzsch STA 449F3 instrument
2 and the weight loss in function of temperatures between 105°C – 1000°C was recorded.

3 **3.2. Mix design of CEB**

4 The principle and the process of CEB production consists of using raw material compacted
5 and mechanically shaped. In order to evaluate the compaction properties of representative
6 clays, various compression tests were carried out. The test consists of mixing and
7 homogenizing all dry components (clay, sand, lime), and then a sustainable amount of water
8 is added to manufacture the paste of bricks. Obtained mixtures were extruded into cylindrical
9 test specimens (50 mm of diameter and 100 mm of high).

10 Pressure of 20 MPa allows to compact mixture using a specific mold in order to obtain
11 homogeneous and well stabilized samples. Unconfined Compressive Strength (UCS) was
12 measured according to standard [NF P 98-232.1 \[11\]](#), using an Instron 300 DX model-testing
13 machine, connected to a Partner TM Testing Software. Failure of test piece makes the end of
14 UCS test; ramp speed used was 11.78 kN/min. Stress and strain were automatically registered.
15 Compaction used for specimens was static compaction with simple effect type, ensured by
16 means of a hydraulic press. The lower plate of press moves while the assembly (mold +
17 mixture + piston) and the upper plate remains fixed. The operation was conducted until
18 desired compaction stress is reached. During all stages of this study, mixtures were subjected
19 to a compaction stress of 20 MPa. After demolding test pieces, the diameter, height and mass
20 of each specimen were immediately measured. After shaping, a drying phase in furnace at
21 60°C for 7 and 28 days was necessary, in order to remove residual water in the produced
22 bricks. Subsequently, molds manufactured were subjected to different mechanical tests [\[12\]](#).

23 During this work, an experimental study of raw earth materials behavior was carried out. Two
24 formulation steps were studied: (a) the first was to look for granular matrix (mixture
25 composition) in order to achieve the most effective mechanical resistance. (b) The second was
26 to study mechanical properties reinforced by adjuvants. This additive allows to improve final
27 product properties. Indeed, lime stabilization is a process that chemically improves many
28 characteristics of soils especially compressive strength. The influence of several parameters
29 has therefore been tested on mechanical behavior of the products obtained.

30 **4. Experimental Results**

31 **4.1. Characterization of raw clay samples and position with respect to CEB** 32 **recommendations**

1 4.1.1. Particle size distribution data

2 Particle size distribution presents one of the main criteria in manufacturing suitable earth
3 blocks. Fig. 2.a shows the particle size distribution of natural clay, sand as well as the
4 recommendation range deduced from the CEB norms NF XP P13-901 [13].

5 Granulometry curve of natural clay was beyond the range because they were much finer.
6 Thus, sand 0/ 2 mm was added. Data obtained showed that the new granulometry curve of
7 mixture was well positioned on the recommendation range (Fig. 2.b).

8 Table 1 presents the composition of cohesive soil for three samples. Results show that 13.77,
9 19.62 and 9.62 % of Clay, 58.14, 46.48 and 27.7 % of silt and 28.09, 33.9 and 63.11 % sand
10 compose samples A1, A2 and A3, respectively. Therefore, sample A3 had the coarsest
11 fraction. The presence of high fraction of silt gives the material an importance for the
12 construction field. This fine fraction given by clay plays an interesting role in building as it
13 fills the voids created by the sand (coarse fraction), resulting in a denser mix [2].

14 The sand formulation used comprises 2.07% clay, 6.72% silt and 91.21% sand. Fineness
15 modulus of sand is 2.29, which characterizes an optimal sand referring to NF EN 933-1 (2.2
16 $<M_f < 2.8$) [14].

17 According to results (Table 1) revealed by the curvature coefficient C_c and C_u ($1 < C_c < 3$ and
18 $C_u < 2$). These materials are dense, well graduated and have uniform particle size [15, 16].

19 Helium pycnometer method confirms geotechnical results, the sample A1 ($\rho = 2.77 \text{ g.cm}^{-3}$)
20 was denser than A2 ($\rho = 2.63 \text{ g.cm}^{-3}$) and A3 ($\rho = 2.57 \text{ g.cm}^{-3}$). The density of the sand used is
21 2.65 g.cm^{-3} .

22 4.1.2. Atterberg limits

23 Fig. 3 show the plasticity chart by Casagrande and the plasticity index that is represented in
24 the diagram proposed by norm NF XP P13-901. Low swelling behavior characterized A1 and
25 A2 samples. Therefore, these clays A1 and A2 are considered non-plastic, in the way it is easy
26 to dry and have a good optimization of block fabrication. Soils A1 and A2 had a low plasticity
27 index value, which indicates their low clay content and the abundance of quartz.

28 Results also show that these clays have low shrinkage that is appropriate for blocks
29 production ($W_r < 12$) [7, 8]. Soils can be considered, according to plastic index, as solid state
30 ($W < W_p, I_c > 1, II < 0$) for all samples.

31 4.1.3. Chemical identification

32 Chemical analysis indicates that samples were rich in silica, alumina and alkalis. The SiO_2
33 content was up to 50% (m %) in all studied samples, as the Al_2O_3 values ranged from 18 to

1 20% (wt %). As shown in [Table 2](#), mass ratio $\text{SiO}_2 / \text{Al}_2\text{O}_3$ values are higher than the classic
2 value founded in pure kaolinite ($\text{SiO}_2 / \text{Al}_2\text{O}_3 = 1.18$) and montmorillonite ($\text{SiO}_2 / \text{Al}_2\text{O}_3 =$
3 2.36) [[17](#)]; due to the quantity of quartz present. Lime content was reactively low in all
4 samples that confirm current objectives and CEB production. This amount was high for clay
5 A3 (calcium clay). According to [Jamoussi et al., 2003](#)[[18](#)], the clays have high content of K_2O
6 ranging between 2.53 and 6.38% due to the presence of illitic phase.

7 Loss on Ignition (LOI) is determined by calcination powders up to 1000°C . The high LOI was
8 associated to the presence of carbonates and the bound water evaporated by heat treatment.
9 This result explains the test water content of each sample, as well as the large capillary
10 retention due to its large surface area. LOI content values were 5.07, 6.42 and 12.24 for
11 samples A1, A2 and A3. It is noted that clay A3 was the wettest. These high content values
12 can be explained by a significant proportion of kaolinite.

13 *4.1.4. Specific surface area analysis*

14 Nitrogen adsorption-desorption isotherms recorded on the clay materials (A1, A2 and A3) are
15 presented in [Fig. 4](#). For these representative clays, isotherms were of type IV isotherm
16 according to the IUPAC classification, which is characteristic of porous adsorbents having
17 pore sizes in the range of 70-100 Å [[10](#), [19](#)]. The superposition of adsorption and desorption
18 curves shows the absence of internal mesoporosity of the sample, especially for clay A1. The
19 presence of internal and inter-granular pores and the hysteresis is explained by the internal
20 porosity of the material. Indeed, the more the number and the pore size increases, the specific
21 surface area becomes higher [[10](#), [20](#)].

22 Values of specific surface area vary between 22.46, 63.4 and 64.22 m^2/g for A1, A2 and A3
23 samples, respectively. The sample (A1) had a smaller specific surface than A2 and A3, due to
24 its microstructure. Type of clay, minerals associated and the dominance of illite and kaolinite
25 phases influenced the results [[18](#)].

26 Consequently, with Pycnometer test, values of porosity and porous volume are in agreement
27 with the precedent analysis. The internal porosity values were of 50.46, 44.37 and 38 % for
28 A1, A2 and A3, respectively. The porous volumes are 0.37, 0.35 and 0.29 $\text{cm}^3 \cdot \text{g}^{-1}$ for A1, A2
29 and A3, respectively.

30 *4.1.5. Optical microscopy and SEM characterization*

31 Optical microscopy and SEM allow observing the sample surface's topography; it provides
32 detailed surface data of solid samples. [Fig.5](#) displays textural characteristics of clay samples
33 obtained by SEM analysis. SEM images show that the samples A2 and A3 have a

1 discontinuous structure and an open texture with the presence of visible and connected voids.
2 Soil A1 presents a compacted microstructure, with the presence of a porous structure, which
3 could provide a high value of porosity and a high adsorption capacity. Clay A3 contains the
4 coarse fraction compared with A1 and A2.

5 *4.1.6. Mineralogical identification*

6 The mineralogical structure of various natural clay samples was studied [9, 21]. According to
7 Fig. 6, Kaolinite, illite and smectite are the main clays present in the materials.

8 The centrifugation technique allows separating minor fraction from each sample. Samples
9 placed into oriented blades were scanned in air-dry state, treated by glycol solvation and
10 heated at 550°C. The most mineralogical phases identified were Illite, Kaolinite, Smectite and
11 Quartz.

12 The presence of kaolinite phase was confirmed by the presence of the reflection at 7 Å
13 (powder) and that disappears after heating at 550°C: kaolinite is transformed into metakaolin
14 above 450°C. Smectite was clearly identified by comparing diffraction patterns of air-dried
15 and ethylene glycol EG solvated. Kaolinitic phase contributes to good drying characteristics
16 of materials [4]. The mineralogical composition of the clays consisted of 13.58% Kaolinite
17 (K), 25.7 % illite (I), 11.82% smectite (S) and 48.90% quartz (Q) and impurities for A1. The
18 clay A2 is composed of 25.3 % K, 45.83 % I, 38.9% S and 24.98 % Q, while A3 is formed by
19 38.34 % K, 24.89 %I, 18.74 %S and 18.03% Q.

20 Kaolinite is the most used mineral for CEB manufacture. Quartz is always associated with
21 kaolinite. The presence of kaolinite minerals contributes to good shaping, ameliorates
22 plasticity properties and limits the drying properties. In contrast, Smectite phase increases
23 moisture content as shown in sample A3. This contributes to shrinkage phenomena [21]. The
24 soil A1 is composed of a high rate of quartz that explains low plasticity as demonstrated.

25 *4.1.7. FTIR analysis*

26 The infrared spectrum shows the presence of several characteristic absorption bands in the
27 infrared region 4000 to 400 cm⁻¹. Results are shown in Fig. 7. The identification of soil
28 minerals by FTIR analysis is determined by reference to spectra (Farmer, 1968) [18, 23, 24].

29 FTIR spectra patterns showed heterogeneous mixtures of clay components and differences in
30 their composition and structure. First, infrared absorption properties of kaolinite
31 corresponding to OH bands were established at 3563.33 cm⁻¹ for A1, 3624.15; 3611.79 cm⁻¹
32 for A2 and 3645.37 cm⁻¹ and 3611.79 cm⁻¹ for A3. In addition, specific bands of
33 accompanying mineral were observed (presence of kaolinite form and quartz) at 952.32 cm⁻¹

1 for A1, 974.69 and 687.69 cm^{-1} for A2 and 989.60, 907.60 and 687.69 cm^{-1} corresponding to
2 clay A3. The quartz was detected at 775.28, 780.87 and 777.14 cm^{-1} for A1, A2 and A3
3 respectively. The band at 1625.12 cm^{-1} for clay A2 is attributed to the presence of an
4 amorphous alumino-silicate OH group. These results confirm and corroborate the XRD data.

5 *4.1.8. TDA/TGA analysis*

6 Water evaporation and carbonate decomposition are the most significant weight loss
7 processes in CEB manufacturing. According to research work of [Aras and Farmer \[21, 23\]](#),
8 thermal analysis of raw materials and weight loss represented in [Fig. 8](#) could be due to the
9 same process.

10 In clay materials, some reactions are responsible for mass loss as H_2O and organic materials.
11 A first endothermic peak was depicted at low temperature ($< 150^\circ\text{C}$ for all clays studied); this
12 loss is attributed to moisture elimination and absorbed water departure, and consequently the
13 loss of weakly bound water. Mass loss around 520°C is due to the removal of water content
14 from clay minerals indicating the dehydroxylation reaction. The decomposition of carbonates
15 (740°C) was detected only in the structure of clay A3.

16 Total weight loss of A1, A2 and A3 were 4.7 %, 8.69 % and 14.51 % respectively ([Fig. 8](#)).
17 The greatest mass loss was obtained in sample A3; which is in a good agreement with its
18 chemical and mineralogical composition (LOI and alkaline oxides content).

19 Moisture or water contents can be directly measured using a known volume of the material,
20 and a drying oven. Values obtained were 2.47, 4.3 and 7.46 for A1, A2 and A3, respectively.

21 Results based on mineralogical, chemical and physical characteristics, show that the raw clays
22 studied display an interesting potential for CEB.

23 **4.2. Potential application**

24 The influence of several parameters was tested on the mechanical behavior of the products
25 obtained. For three types of clay selected, it was interesting to study different factors: water
26 content, mixture composition and setting time, in order to evaluate the variation of mechanical
27 properties and achieve the optimal compressive strength. [Table 3](#) summarizes the
28 formulations and the quantities of materials used for each block series.

29 After remolding test pieces, some blocks presented a heterogeneity on their surface due to the
30 difference of mixture constituent's particle sizes ([Fig. 9](#)). After drying for 7 days, none of the
31 blocks, even with calcined clay A3 had a trace of efflorescence, an aesthetic problem due to
32 the presence of white spots on the surface of specimens.

1 The clay behavior under static compaction test was used in order to study the impact of
2 compression load on compacted earth properties. The compaction energy is an important
3 element in static compression test. This process measures the amount of energy based on
4 properties of soil and the amount of water content. Mechanical behavior of blocks in
5 compression was characterized through displacement-controlled uniaxial tests (Fig.10 (a), 10
6 (b)).

7 Displacement in compression (dh) for wet soil is shorter than dry soil. Indeed, a soil with high
8 water content reaches dh faster compared to low water content. Water content influences
9 sample displacement in mold test tube height. So, increasing water content fosters the
10 saturation of soil, (Fig. 10 (a)), therefore pores are saturated and pore volume is reduced
11 during compaction (Fig. 10 (e)). Lime addition into materials consumes much time (difficulty
12 of settlement) to be compacted than untreated samples (Fig. 10 (b)). Displacement in
13 compression of sample with lime is slower: lime densifies the material, flocculates and
14 coagulates clays, then absorbs water and fills voids (Fig. 10 (f)). However, the variation
15 remains associated with the type of clay and differs according the character of swelling. That
16 is why it shows some differences in the three types of soils especially soil A3 that contains an
17 important percentage of smectite phase minerals.

18 The mechanical behavior of blocks in compression was characterized through displacement-
19 controlled uniaxial tests and behavior curves (stress-strain). Fig. 10 (c), 10 (d) shows the
20 behavior of material defined by two states: a linear state and a softening state. For weak
21 deformations, a linear elasticity and a rigid behavior characterize the materials. The pre-peak
22 region is relative to small deformations compared to total deformation. The post-peak region
23 called softening zone results in a loss of bearing capacity of specimen without thereby
24 fragmentation. It is remarkable that the peak or maximum of shear stress corresponds to the
25 fracture of specimens. Beyond the peak (ultimate strength), stress decreases, then there is an
26 inflection point of post-peak curve where deformations become significant compared to stress
27 drop Fig. 10 (c), 10 (d). Strong materials (with low water content and with lime added) can
28 support high tensile force compared with weak materials that broke very quickly as presented
29 in Fig.10 (e), 10(f)). Addition of lime makes the blocks more resistant [26, 27, 29].

30 Density is the key indicator used to classify solid construction blocks. Compressive strength
31 of earth blocks samples depend on their density. After compacting final height (H_f) and wet
32 mass (M_h) of test pieces are measured. These data allow calculating dry density of specimen.
33 A material with high water content needs less energy to achieve the same dry density (γ_d)

1 since water plays the role of lubricant. Compacting wet soils consumes less energy compared
2 to dry one, as the frictional dissipation is more important. As water content increases,
3 saturation of soil increases and therefore pores are saturated and pore volume is reduced
4 during compaction.

5 The rate of adjuvant increases samples' density as presented in Fig. 11. The increase in
6 maximum dry density is a reliable indicator of clay improvement. Results demonstrate that
7 the weight of samples fell remarkably high, due to the increasing number of voids formed
8 within blocks by the highly porous clay particles. Increase in density is attributed mainly to
9 the filling of voids between soil particles and natural pozzolan as the latter has a higher
10 specific gravity.

11 Most of density values obtained were justified by Delebecque R and Guilaud H [29, 30]; in
12 the range of 1.7 and 2.2 g.cm⁻³ (Fig. 11). The maximum dry density acquired was due to
13 particle size and specific soil surfaces.

14 For the production of CEB, the specimens were tested and characterized at a laboratory test.
15 Weight loss, drying shrinkage, porosity, packing density as well as the compressive strength
16 were determined.

17 4.2.1. Weight loss

18 Mass loss is due to departure of added water. It is calculated from the following formula.

$$19 \quad LM = (M_i - M_f / M_i) * 100$$

20 M_i: Initial mass before drying

21 M_f: mass after drying

22 Table 4 presents the result of weight loss of samples. Increasing water content leads to further
23 mass loss. In fact, the material becomes wetter and then excess water is released. Mass loss
24 increases with also setting time because an important amount of water evaporated. Therefore,
25 with more drying time in the oven, material still loses its mass and becomes more resistant
26 (Table 4 a).

27 Mass loss for clay A3 was more important than A2 and A1; this result is related to chemical
28 analysis, loss on ignition, moisture content and TGA curve analysis (heat release and H₂O
29 peaks). A3 also contains a high quantity of smectite and requires significant water content.

30 Lime addition makes mass loss very important. In fact, lime closes pores and fills voids.
31 Decreasing void rate between grains makes resistance rather significant and hence the

1 mechanical strength (Table 4 b). To conclude, soils A1, A2 and A3 have a different behavior
2 depending on the moisture content.

3 Fetra et al (2016) confirmed this result and explained it by high porosity of hydraulic lime that
4 allows excess moisture to be released instead than stores it inside. Excess moisture captured
5 inside materials in building is unhealthy. In fact, we use hydraulic lime for the simple reason
6 of allowing building to 'breathe' [31].

7 4.2.2. Drying shrinkage

8 Drying shrinkage is a key parameter in measuring the quality of the CEB. It reflects an
9 expansion/contraction behavior. The test is responsible on the capacity of clays to release or
10 store water [32]. The drying step is very important as it avoids cracking of the samples.
11 According to the results obtained (Table 4), the shrinkage percentage depends on clay type
12 and give us an idea about the important amount of water evaporated [32]. High shrinkage
13 value are disturbed for clay rich in CaCO_3 . In fact, volumetric shrinkage depends on flux
14 materials, the percentage of mixing water and the decomposition of gaseous phases. Flux
15 materials could fill voids and compress between spaces, in against part, gases generated could
16 be generated pores [33].

17 The shrinkage value of the manufactured blocks decreased linearly with the lime
18 supplementation (Table 4 b). This is due to the increase in the initial moisture content present
19 in the clay mixture with the lime addition. Thus, obtained product incorporated with lime
20 could be further evaporated because of the organic matter present, which causes the expansion
21 phenomenon and lower shrinkage.

22 4.2.3. Porosity and packing density

23 Understanding the behavior of a mixture requires the knowledge of its packing density. Data
24 of porosity and packing density are shown in Table 5, where the sum of porosity and
25 compactness is equal to 1. The ratio between absolute density and bulk density refers to
26 compactness.

27 Porosity affects significantly the mechanical properties, durability, and water absorption. A
28 high water content leads to increasing porosity and the structure becomes less compact and
29 less dense. Lime, due to its porous character, allows to fill voids, then densifies the material
30 and increases its packing density.

31 Generally, organic matter decomposition generates small pores in the matrix. Fluxing agents
32 (Fe_2O_3 , K_2O , MgO , CaO and Na_2O) play a key role in the porosity [33, 34]. Sources of
33 fluxing agents like K_2O , Na_2O and Fe_2O_3 allow densifying clay. As shown in clay A1 and

1 A2, important values of flux materials (K_2O , Na_2O_3 and Fe_2O_3) compared to clay A3 led to
2 the densification of particles, thus particles close together. Besides, for A3, high content of
3 CaO and MgO act as pore generating agent. Therefore, increased porosity was observed for
4 specimens leading to decrease of mechanical strength properties. [Table 5](#) show some
5 differences in values of porosity of three types of soil studied. The different values of porosity
6 are also due to the amount and size of pores. In conclusion, as shown, less void volume
7 (reduced porosity) was associated with compact and dense structure, higher strength and
8 therefore better quality.

9 *4.2.4. Mechanical strength*

10 Compressive strength is the most important parameter of construction blocks. Compression
11 tests were carried out using an ISTRON type mechanical press (the same used during the
12 testing of specimens).

- 13 • Mixture composition effect

14 The difference in compressive strength is very clear and varies with different raw material
15 rates. Indeed, for a maximum resistance, the optimum mixture chosen was 70% sand / 30%
16 Clay ([tab. 6](#)).

- 17 • Water content effect

18 According to data collected, unconfined compressive strength for specimens cured after 28
19 days are higher than after 7 days as presented in [Fig. 12](#). For different mixtures prepared, it
20 can be seen that an increase in water content caused a decrease in the compressive strength
21 values after 7 and 28 days. Indeed, the presence of water in specimens weakened their
22 resistance. Furthermore, water content was evaporated with the setting time, so compressive
23 strength increased. Setting time allows occupying and filling voids and pores into blocks
24 creating then a dense structure. The less void volume is related with higher strength and
25 therefore better quality [[35](#), [36](#), [37](#)].

- 26 • Effect of lime added

27 Stabilizing soil is very important in manufacture of CEB in order to ensure good mechanical
28 properties. In general, lime can be an excellent choice to treat soils. The advantage of this
29 stabilizant is related to its low quantity added and its ecological use. The reaction between
30 lime and clay produces stable calcium silicate [[2](#)].

31 A Natural Hydraulic Lime NHL with 3.5 MPa (moderately hydraulic) was used; this type of
32 hydrated lime is highly required for soil stabilization. The hydraulic lime properties has
33 characterized by a slow setting time and a good compressive strength [[36](#)]. Hydraulic lime is

1 recommended because it allows absorbing carbon dioxide from air and having low plasticity
2 that hinders the formation of cracks [38].

3 According to data obtained (Fig. 13), values of compressive strength are better for stabilized
4 soil with lime compared with untreated soil. The addition of lime as adjuvant improves
5 mechanical properties of the material. Lime slow reaction and the quality of earth explained
6 this result [39, 40]. Values of compressive strength obtained are in correlation with some
7 researches such as Delebecque R and Guilaud H [26, 27].

8 To conclude, there are two main modes of lime treatment to improve performance of earth
9 materials, which are structure modification and stabilization. In fact, these modes can upgrade
10 mechanical strength of soils. In the first reaction, the process makes the flocculation and
11 agglomeration of clay minerals leading to a reduction in plasticity and moisture content. This
12 phenomenon also contributes to changing clay texture and improves consistency of treated
13 clay soils.

14 Lime dissolution in soil allowed the saturation of calcium. Clays released alumina and silica
15 that react with calcium to form calcium hydrates CSH. A pozzolanic reaction and a
16 cementitious product were formed with good mechanical properties. Adding lime to a reactive
17 soil formed stable calcium silicate hydrates CSH that in turn explain the increase of
18 resistance. Then, mixing lime with clay caused hydration of clay particles by fixing a quantity
19 of water to make a more granular and resistant structure [31, 39, 40].

20 Lime effect was very dependent on nature and type of clay used. In fact, compressive strength
21 was a function of clay variety. In fact, lime reacts much faster with montmorillonite clays than
22 with Kaolinite, thus reducing plasticity for the first and having little effect on the plasticity of
23 Kaolinites. Lime modification showed increase in strength for expansive (kaolinite) better
24 than expandable clay (montmorillonite) [37]. In view of this, we can conclude that an increase
25 in compressive strength is a function of setting time and the proportion of lime added. The
26 mechanical behavior of the blocks depends on the granulometry, type of clay, water contents
27 and binders. Compressive strength of blocks depends also on their density, porosity and pore
28 size distributions.

29 **5. Conclusion**

30 In this paper, three clays sampled from different geographical locations (Djebel Bouamrane
31 Gafsa, Zeramdine quarry and Djebel Abderahmanne Nabeul) were studied. Mineralogical
32 analysis of samples indicated the presence of illite and kaolinite as dominant mineral phases

1 associated with smectite and quartz. The behaviors of clay bricks depended on the nature,
2 type and the amounts of various minerals present and physico-chemical analysis.
3 Results for manufacturing bricks and Unconfined Compressive Strength were interesting.
4 Earth blocks prepared with different types of raw materials exhibited significant differences in
5 compressive strength values. Performances of clay-sand bricks could be improved by adding
6 an optimum quantity of lime to reach the highest strength. Lime addition reduced the ability
7 of compressed earth to absorb much water; thus, the density increased.
8 Obtained data suggest that potential use of representative clays as raw materials for
9 manufacturing unfired clay blocks. In terms of mechanical properties, better results were
10 given with clay A1, A2 and A3 respectively. A1 was located in the recommendation diagram
11 according to NF XP P13-901 and then confirmed the plastic character. The geochemical
12 analysis showed that the clay fraction had a ratio of $\text{SiO}_2 / \text{Al}_2\text{O}_3$ equal to 3. The SiO_2 content
13 was 57.97% and the Al_2O_3 was 18.71%. The high percentage of K_2O (6.38%) reveals the
14 richness of clay in kaolinite (13.58%) and illite (25.7%). The percentage of CaO confirms the
15 content of loss on ignition (5.07%).
16 Technological tests for bricks A1 stabilized with 10 % lime revealed a weight loss of 10.9%, a
17 porosity of 6.31% and mechanical strength of 7.14 MPa.
18 Despite the low mechanical properties for soil A3, it is remediable to improve strength by
19 granular corrections or adding some green additives.

20
21
22
23
24
25
26
27
28
29
30
31
32
33

1 **References**

- 2 [1] Oti J.E, Kinutihia J.M (2012) Stabilized unfired clay bricks for environmental and
3 sustainable use. *Appl.Clay Sci*, Vol. 58, pp 52-59
- 4 [2] Muntohar A.S (2011) Engineering characteristics of the compressed stabilized earth
5 bricks. *CONSTR BUILD MATER*, Vol.25, pp 4215-4220
- 6 [3] Gouny F, Fouchal F, Pop O, Maillard P, Rossignol S (2013) Mechanical behaviour of an
7 assembly of wood-geopolymer-earth bricks. *CONSTR BUILD MATER*, Vol.38, pp 110-
8 118
- 9 [4] El Fgaier F, Lafhaj Z, Antczak E, Chapiseau C (2016) Dynamic thermal performance of
10 three types of unfired earth bricks. *APPL THERM ENG*, Vol.93, pp 377-383
- 11 [5] Morton T (2005) Unfired earth bricks building. *Building for the future*, pp 24-27
- 12 [6] Oti J.E, Kinuthia J.M, Bai J (2009) Compressive strength and microstructural analysis of
13 unfired clay masonry bricks. *Eng. Geology*, Vol.109, pp 230-240
- 14 [7] Norme NFP 94-051 (1993) Reconnaissance et essais. Détermination des limites
15 d'Atterberg. Limite de Liquidité à la coupelle. Limite de plasticité au rouleau
- 16 [8] GTR-LCPC (1987) Limites d'Atterberg, Limite de Liquidité, Limite de plasticité,
17 Méthodes d'essai. LCPC, Vol.26
- 18 [9] Moore D.M, Reynolds Jr R.C (1997) X-Ray Diffraction and the Identification and
19 Analysis of Clay Minerals. Second ed. Oxford Univ. Press, Oxford
- 20 [10] Lawrence M. A, David R. C (2015) Characterization and Analysis of Porosity and Pore
21 Structures. *Miner. Chem*, Vol. 80, pp 61-164
- 22 [11] French-Standars-NFP-98-232-1 (1991). Tests relating to pavements- Determination of
23 the Mechanical
- 24 [12] Agostino W. B, Domenico G, Céline P.B, Joao M, Nicolas S (2015) Briques de terre
25 crue : procédure de compactage haute pression et influence sur les propriétés mécaniques
- 26 [13]AFNOR NF XP P13-901 (2001) Compressed earth blocks for walls and partitions:
27 definitions Specifications – Test methods – Delivery acceptance conditions.
- 28 [14] AFNOR NF EN 933-1 (1997) Essais pour déterminer les caractéristiques géométriques
29 des granulats - Partie 1 : détermination de la granularité. Analyse granulométrique par
30 tamisage
- 31 [15] NF EN ISO 14688-1 (2003) Geotechnical investigation and testing – identification and
32 classification of soil – part 1 : identification and description

- 1 [16] Delgado M.C.J, Guerrero I.C (2007) The selection of soils for unstabilised earth
2 building: a normative review. *CONSTR BUILD MATER*, Vol.21, pp 237–251
- 3 [17] Cong M, Bing C, Longzhu C (2016) Variables controlling strength development of self-
4 compacting earth-based construction. *CONSTR BUILD MATER*, Vol.123, pp 336-345
- 5 [18] Jamoussi F, Bédir M, Boukadi N, Kharbachi S, Zargouni F, Galindo A.L, Hélène P
6 (2003) Clay mineralogical distribution and tectono-eustatic control in the Tunisian margin
7 basins. *Geosci*, Vol.335, Issue 2, pp 175–183
- 8 [19] Brunauer S, Emmett P.H, and Teller E, (1938). Vol. 60 (2), pp 309–319
- 9 [20] Brunauer S, Emmett P. H, Teller E (1938) Adsorption of Gases in Multimolecular
10 Layers. *Contrib. Bur. Chem, Soils George Wash. Univ*, Vol. 60, pp 309–319
- 11 [21] Aras A, (2004) The change phase composition in kaolinite and illite rich clay based
12 ceramic bodies. *Appl.Clay Sci* 24, pp 257–269
- 13 [22] Farmer V.C (1968) Infrared spectroscopy in clay minerals study. *CLAY MINER*, Vol.7,
14 pp 373–387
- 15 [23] Farmer V.C (1974) The infrared spectra of minerals. *Mineral Sci*, pp 331–365
- 16 [24] Russell J.D, Fraser A.R (1994) Infrared methods, Clay minerals: Spectroscopic and
17 Chemical Determinative Methods. Chapman and Hall, London, pp 11–67
- 18 [25] Vander M.H.W, Beutels P.H (1976). *Atlas Infrared Spectroscopy of Clay Minerals and*
19 *their Admixtures*
- 20 [26] Wheeler S. J, Sharma R. S, Buisson M. S. R (2003) Coupling of hydraulic hysteresis and
21 stress–strain behaviour in unsaturated soils. <https://doi.org/10.1680/geot.2003.53.1.41>,
22 *GEOTECH*, Vol.53, Issue1, pp 41-54
- 23 [27] Chiu F.C.W.W.Ng (2003) A state-dependent elasto-plastic model for saturated and
24 unsaturated soils. <https://doi.org/10.1680/geot.2003.53.9.809>, *GEOTECH*, Vol. 53,
25 Issue9, pp 809-829
- 26 [28] Jian W, Qimin L, Changwei Y, Yidan H.C (2018) A Simple Model for Elastic-Plastic
27 Contact of Granular Geomaterials. *ADV MATER SCI ENG*, Vol. 2018, Article ID
28 6783791, <https://doi.org/10.1155/2018/6783791>
- 29 [29] Delebecque R (1990). *Éléments de Construction Bâtiment*, Edition Delagrave
- 30 [30] Guilaud H (1997) *Centre International pour la Construction en Terre*, Ecole d'Architecte
31 de Grenoble, *Encyclopédie de Bâtiment*, Tome 2 Edition Wake, CRATerre.
- 32 [31] Rahmat M.N, Norsalisma I, Kinuthia J.M (2016) Strength and environmental evaluation
33 of stabilized Clay-PFA eco-friendly bricks. *CONSTR BUILD MATER*, Vol.125, pp 964–973

- 1 [32]mechanical properties of fired-clay bricks incorporating ETP biosolids. Journal of Cleaner
2 Production 119, <http://dx.doi.org/10.1016/j.jclepro.2016.01.094>
- 3 [33] El Fadaly E.A, El- Enany S.A (2015) Lead free Ceramic Cooking ware from Egyptian
4 Raw Materials. I.J. current Microb. Appl Sci, ISSN: 2319-7706 Volume 4 Number 4, pp
5 474-487, <http://www.ijcmas.com>
- 6 [34] Simão L , Montedoa O.R.K, da Silva Paulaa M.M, da Silvaa L , Rafael Falchi Caldatob
7 R.F, de Mello Innocentnib M.D (2013) Structural and Fluid Dynamic Characterization of
8 Calcium Carbonate-based Porous Ceramics. Mater. Res, 16(6) : 1439-1448 © 2013
9 DDOI : 10.1590/S1516-14392013005000147
- 10 [35] Oti J.E, Kinuthia J.M (2012) Stabilized unfired clay bricks for environmental and
11 sustainable use. Appl. Clay, pp 52–59
- 12 [36] Boussen S, Sghaier D, Chaabani F, Jamoussi B, Bennour A (2016) Characteristics and
13 industrial application of the Lower Cretaceous clay deposits (Bouhedma Formation),
14 Southeast Tunisia: Potential use for the manufacturing of ceramic tiles and bricks. Appl.
15 Clay, Vol.123, pp 210-221
- 16 [37] Mahmoudi S, Bennour A, Meguebli A, Srasra E, Zargouni F (2016) Characterization
17 and traditional ceramic application of clays from the Douiret region in South Tunisia.
18 Appl. Clay Sci, Vol. 127-128, pp 78–87
- 19 [38] Riza F.V, Abdel Rahman I, Ahmad Zaidi A.M (2011) Possibility of lime as a stabilizer in
20 compressed earth blocs (CEB). Int. J. Adv. Sci, Eng. Inf. Tech, Vol.1, Issue 6, pp 582-585
- 21 [39] Maskell D, Heath A, Walker P (2014) Inorganic stabilization methods for extruded earth
22 masonry units. CONSTR BUILD MATER, Vol.71, pp 602–609
- 23 [40] Miqueleiz L, Ramírez F, Seco A, Nidzam R.M, Kinuthia J.M, Abu Tair A, Garcia R
24 (2012) The use of stabilized Spanish clay soil for sustainable construction materials. Eng
25 Geol, Vol. 133-134, pp 9–15

26
27
28
29
30
31
32

Figure captions

1
2
3
4
5
6
7
8
9
10
11
12
13
14
15
16
17
18
19
20
21
22
23
24
25
26
27
28
29
30
31

Fig.1. Study area geological setting

Fig.2. Particle size distribution of clay, sand, mixture used and the recommendation range deduced

Fig.3. Atterberg limits of the samples and the recommendation range deduced

Fig.4. Nitrogen adsorption-desorption isotherms

Fig.5. Optical microscope images of studied samples (10×) and SEM of representative samples

Fig.6. XRD of clays deposits

Fig.7. FTIR Spectra of representative clay from studied areas

Fig.8. Thermo-gravimetric-analysis of sample clays

Fig.9. Samples confined aspect

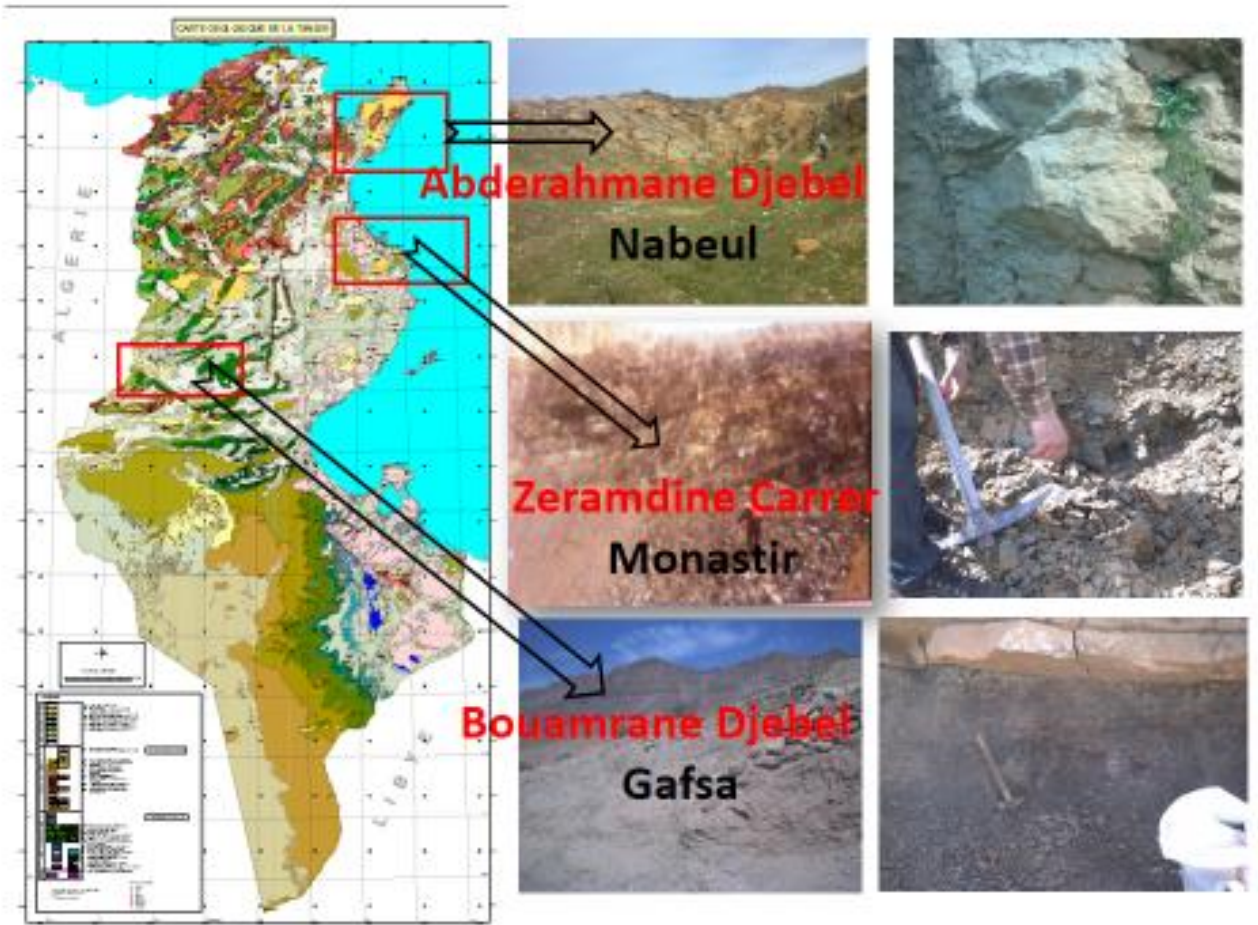
Fig.10. Press experimental result

Fig.11. Density in function of $\log(\sigma)$

Fig.12. Unconfined compressive strength for soil studied

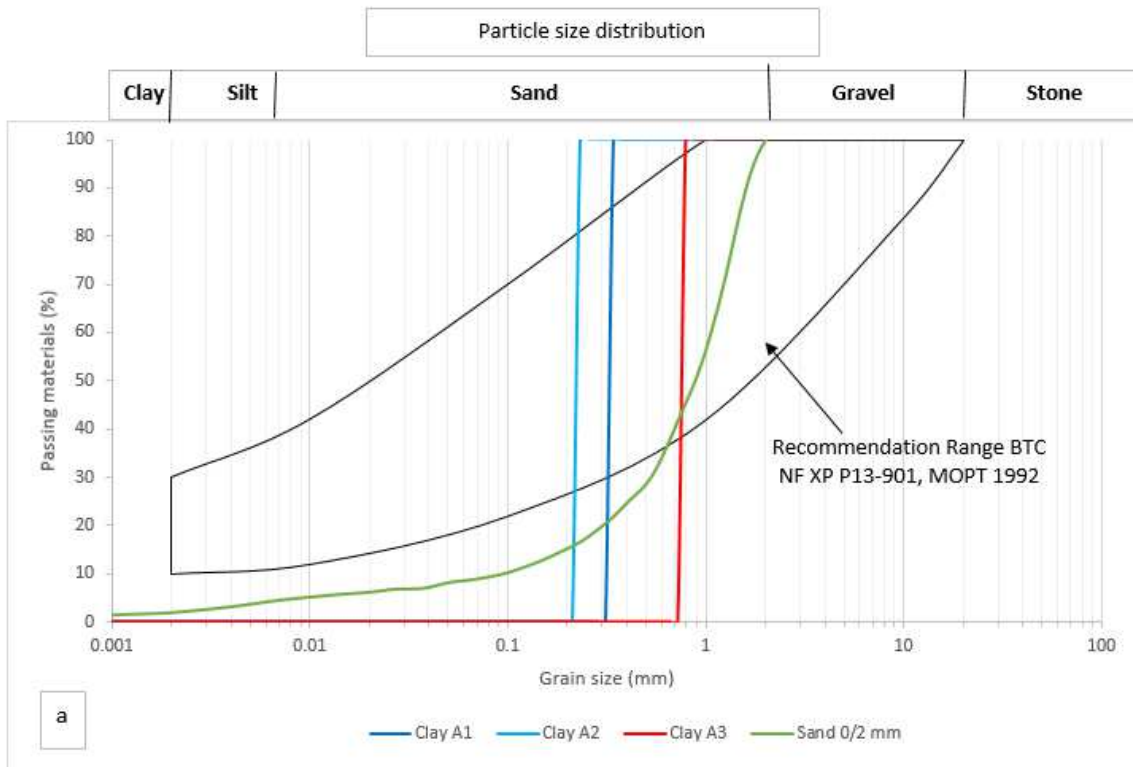
Fig.13. Effect of lime on compressive strength value for soil

1 Fig. 1



- 2
- 3
- 4
- 5
- 6
- 7
- 8
- 9
- 10
- 11
- 12

1 Fig. 2



2

3

4

5

6

7

8

9

10

11

12

13

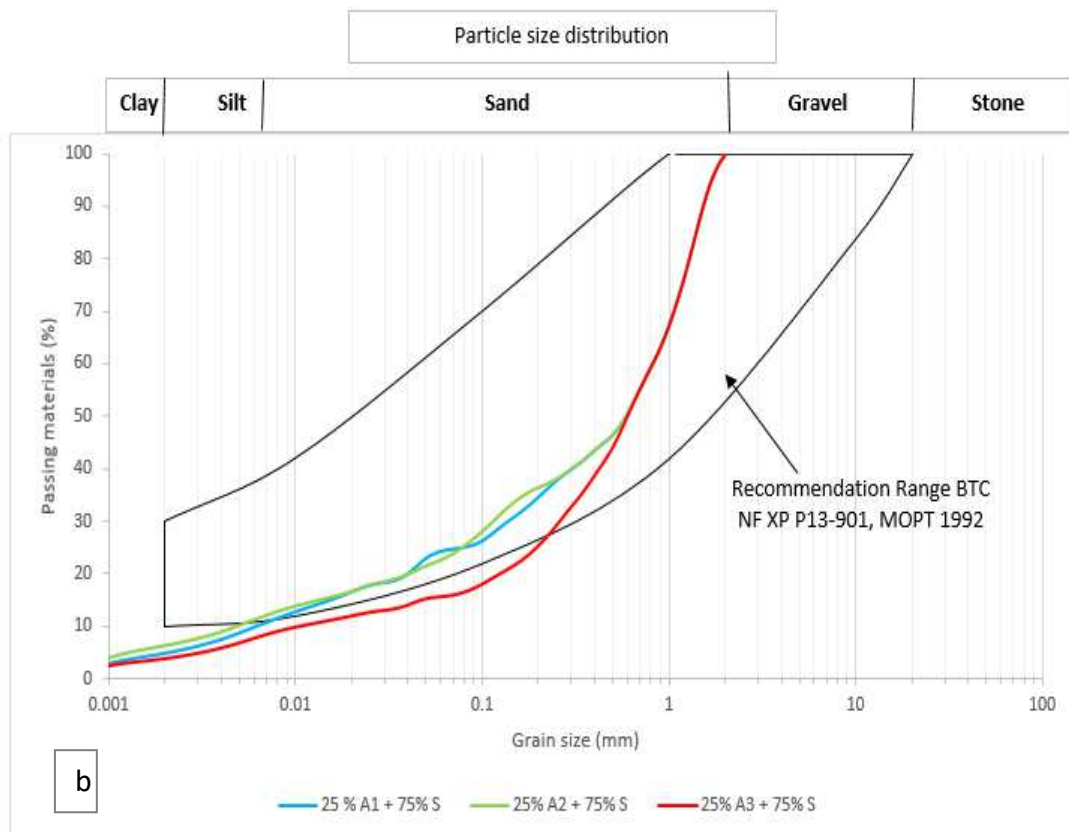
14

15

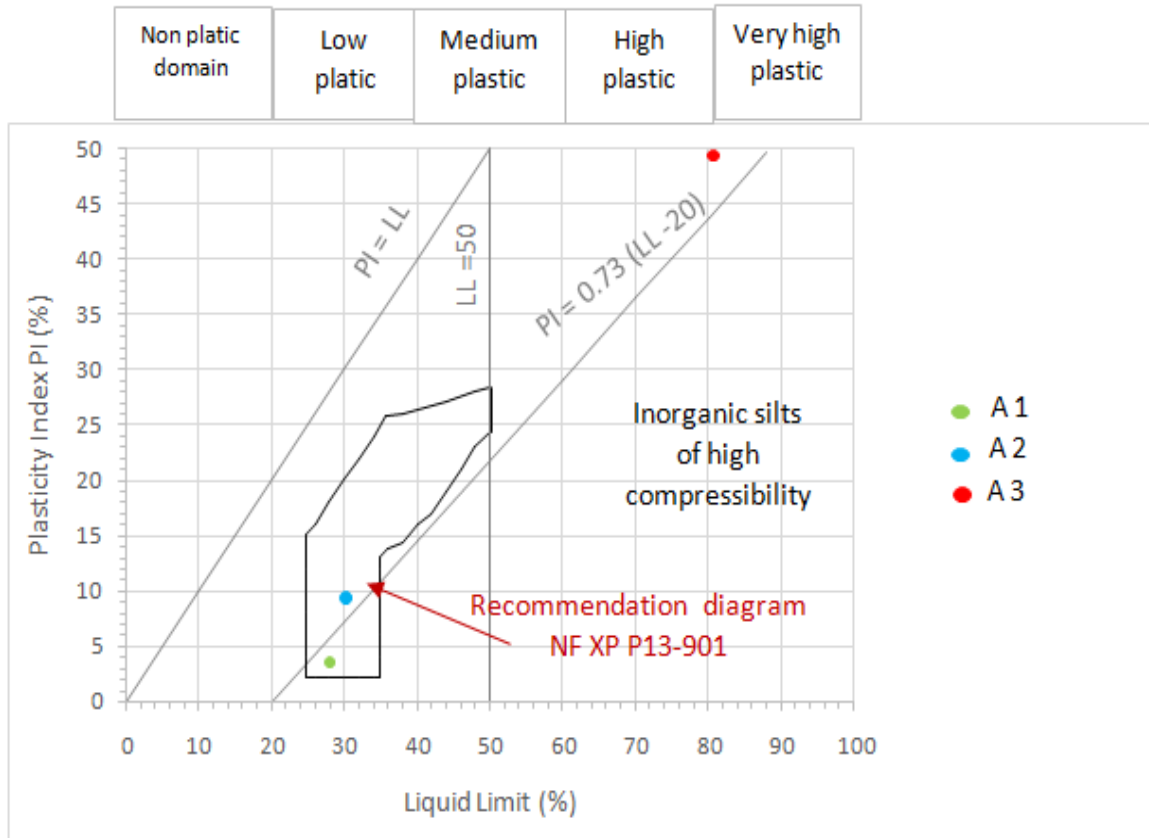
16

17

18



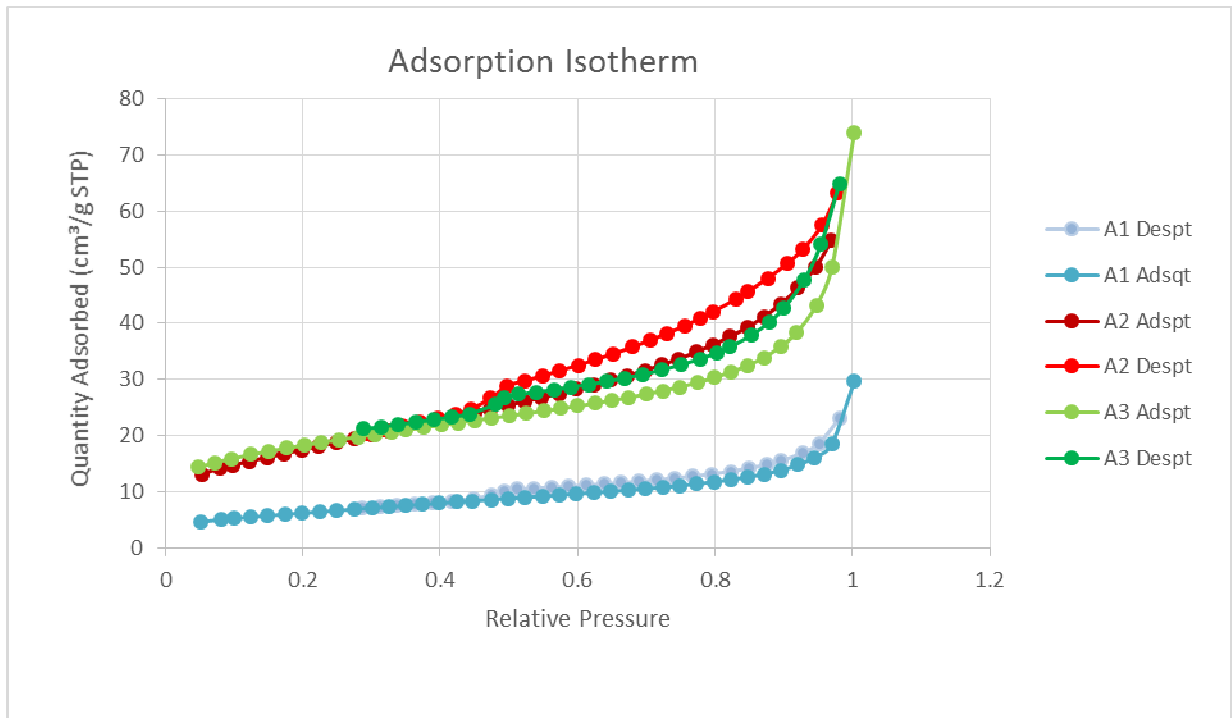
1 Fig. 3



- 2
- 3
- 4
- 5
- 6
- 7
- 8
- 9
- 10
- 11
- 12
- 13
- 14
- 15
- 16
- 17
- 18

1 Fig. 4

2



3

4

5

6

7

8

9

10

11

12

13

14

15

16

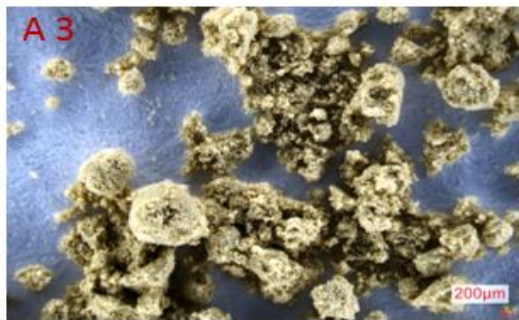
17

18

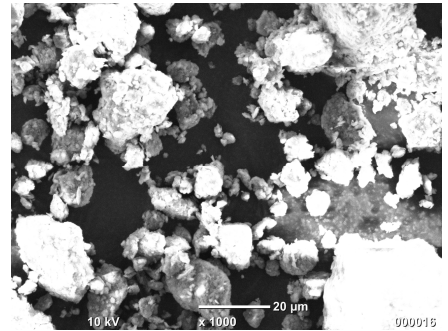
19

1 Fig. 5

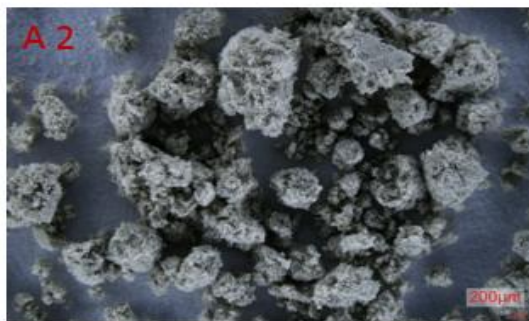
2



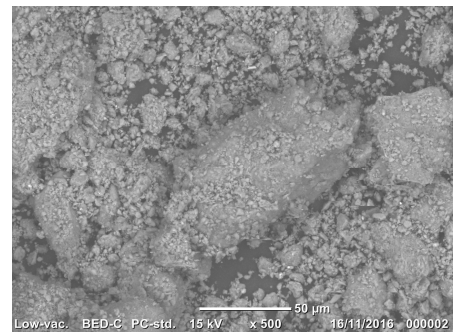
(a)



(b)



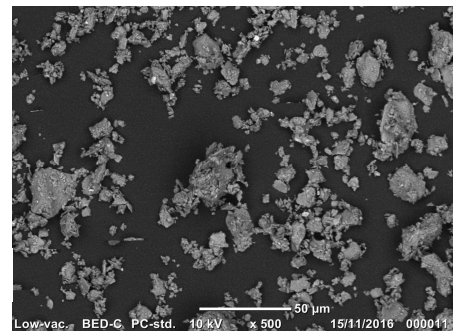
(c)



(d)



(e)



(f)

3

4

5

6

7

8

9

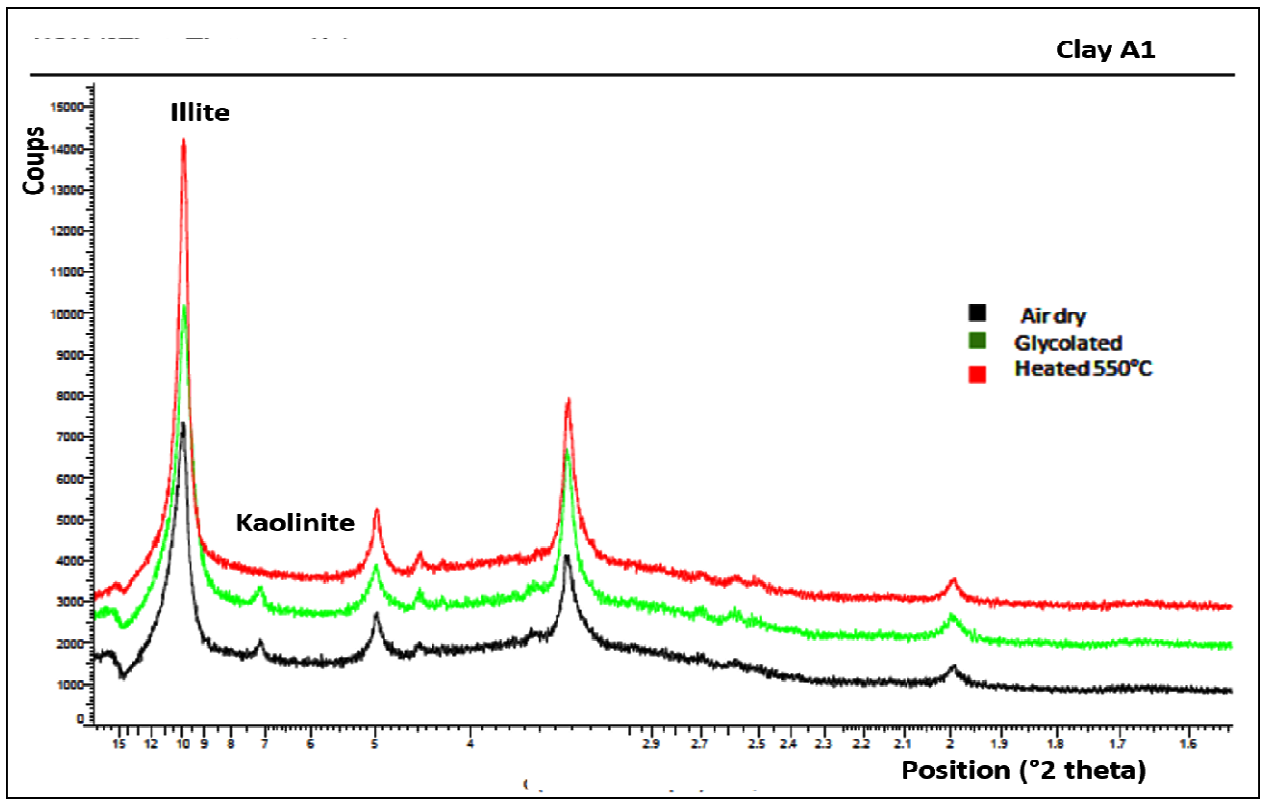
10

11

12

13

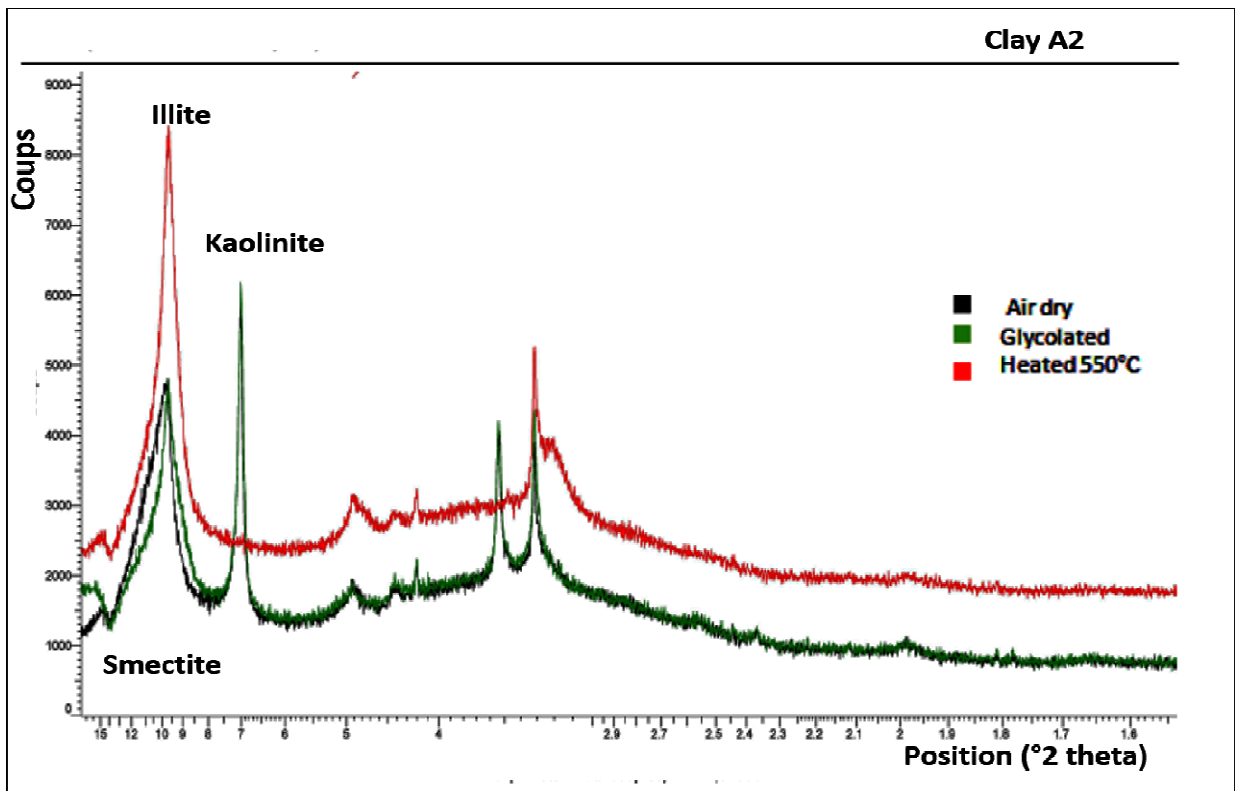
1 Fig. 6



2

3

(a)

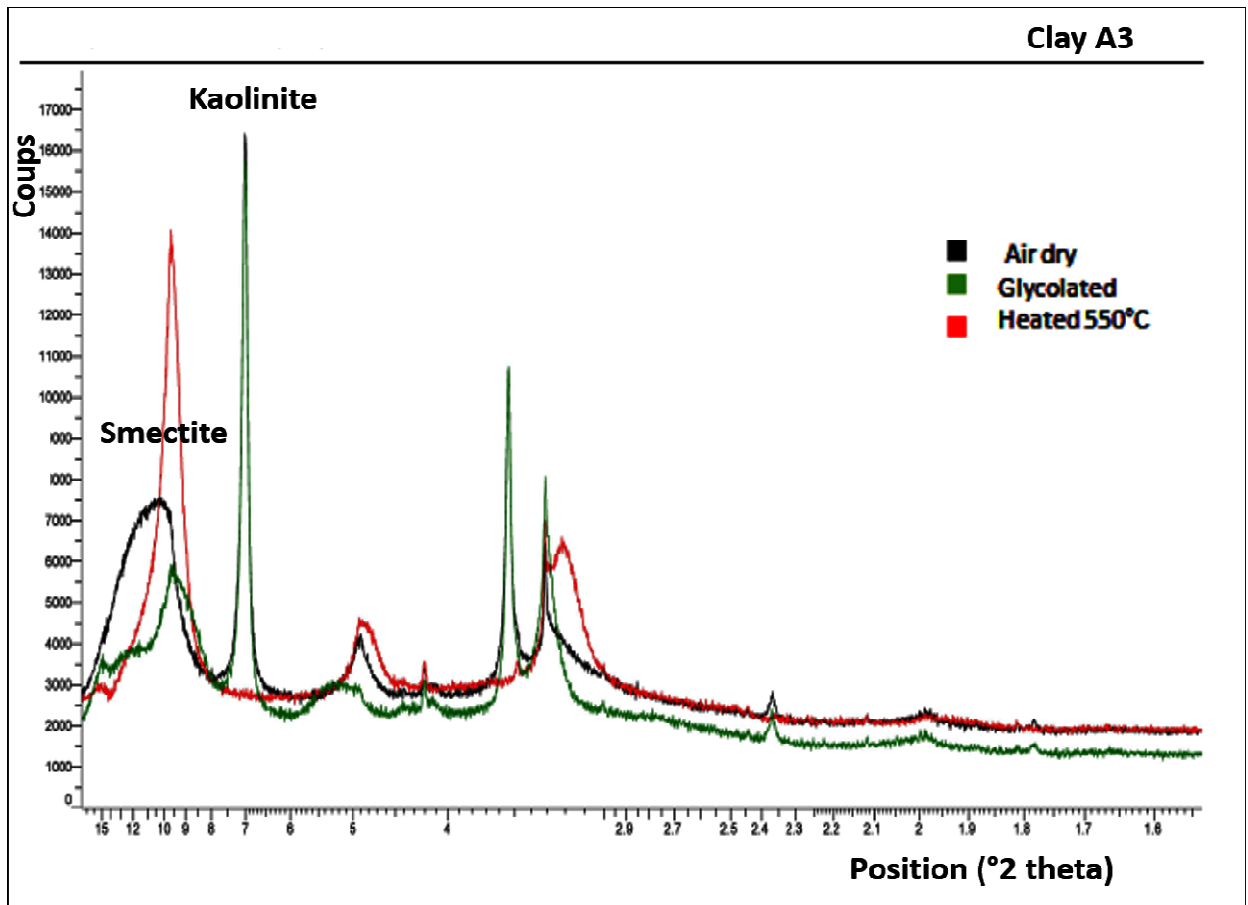


4

5

(b)

1



2

3

4

5

6

7

8

9

10

11

12

13

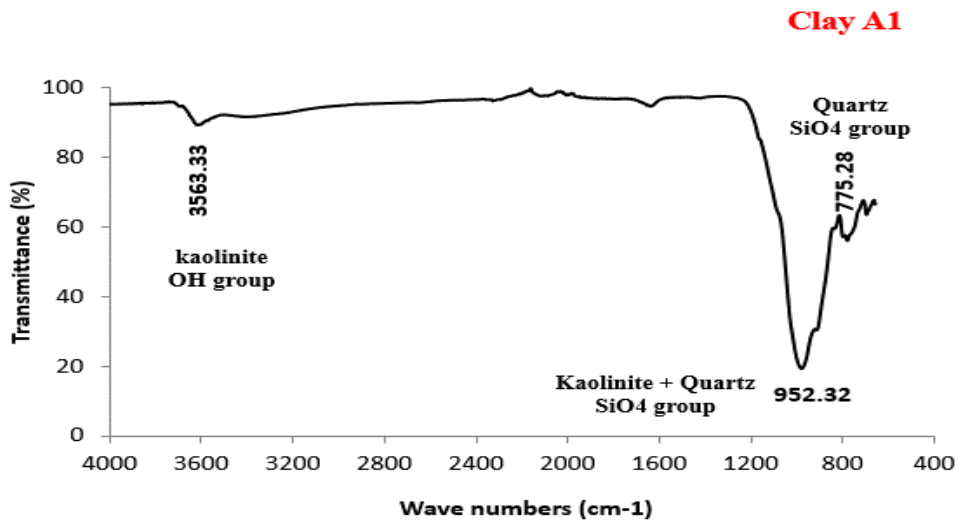
14

15

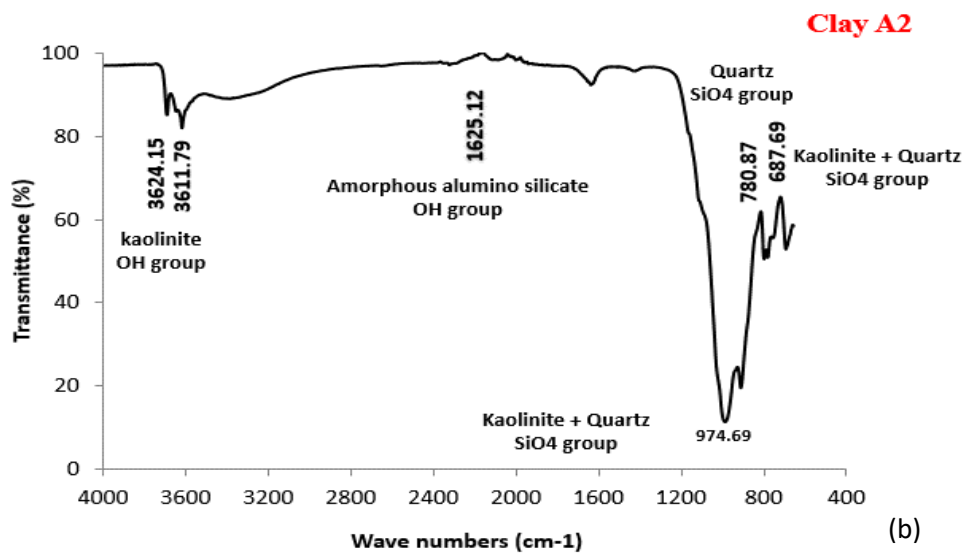
16

(c)

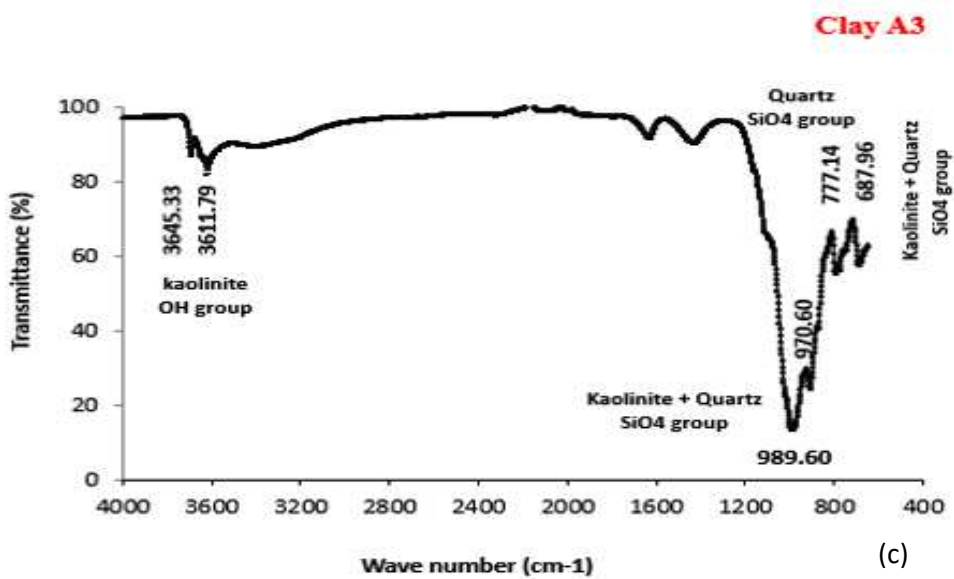
1 Fig. 7



2 (a)

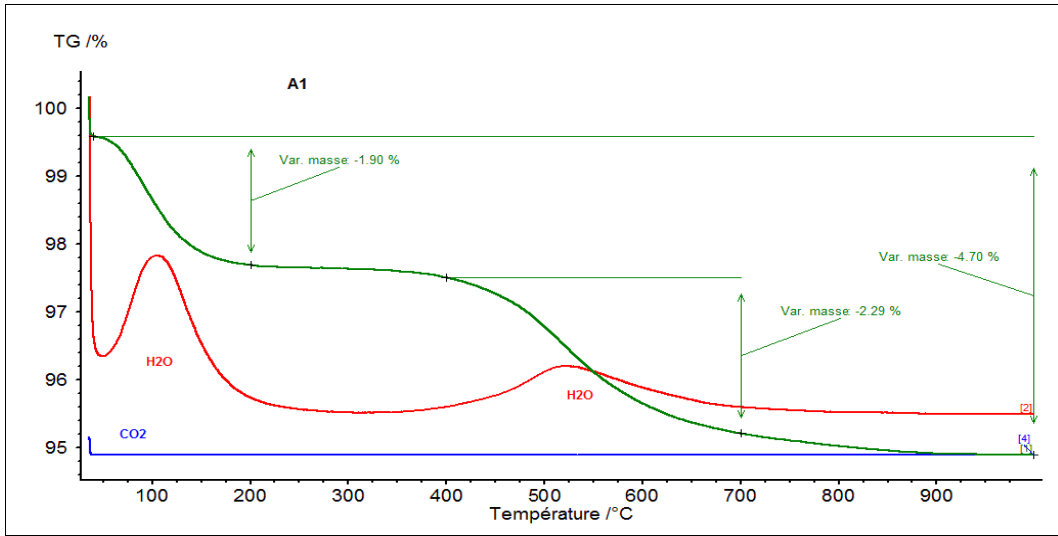


3 (b)

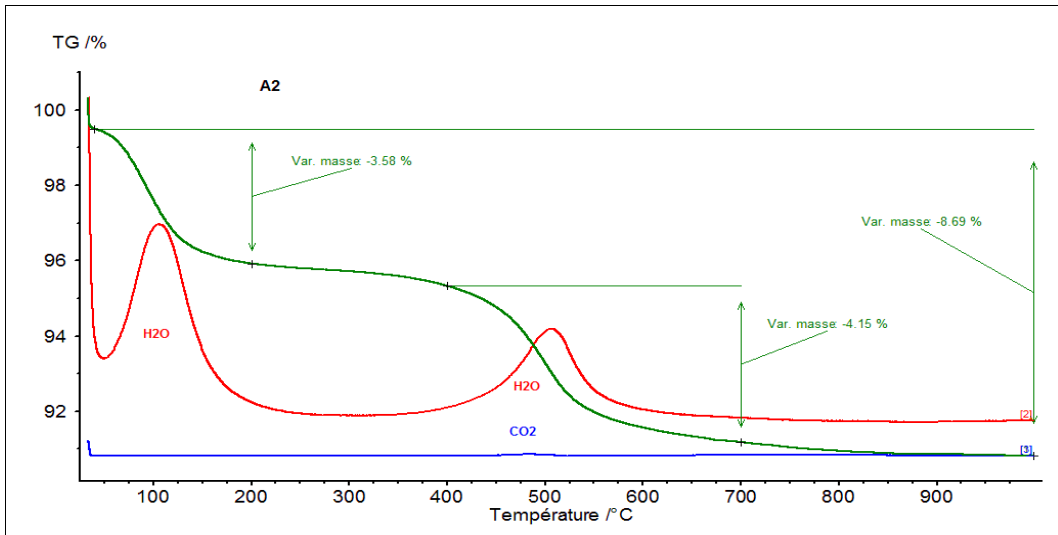


4 (c)

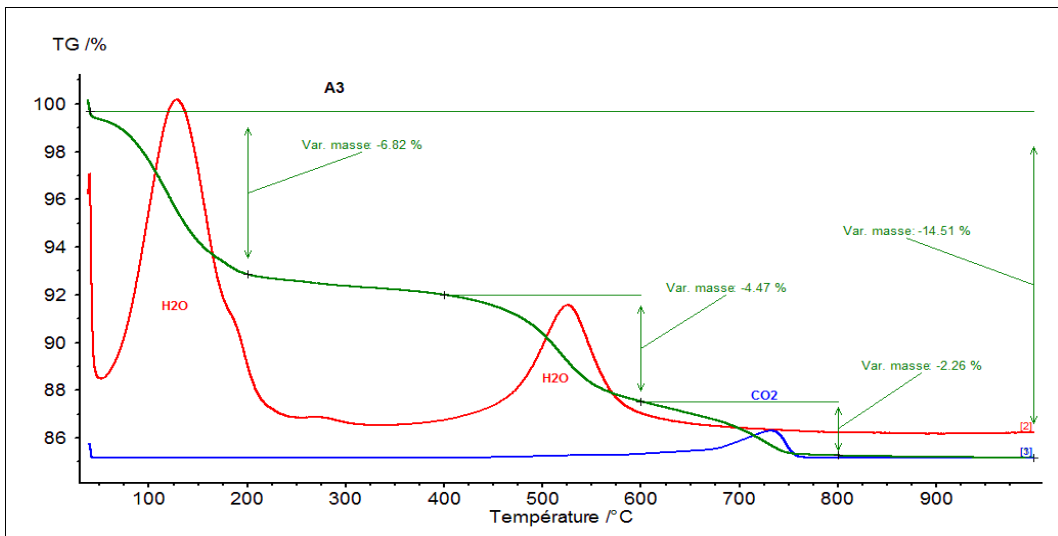
1 Fig. 8



2



3

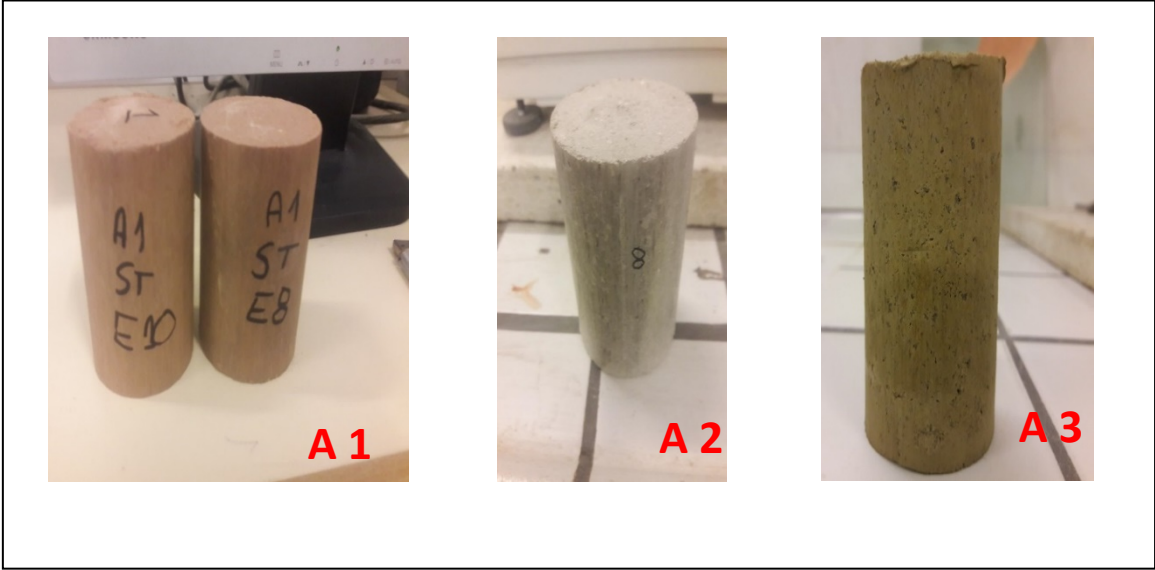


4

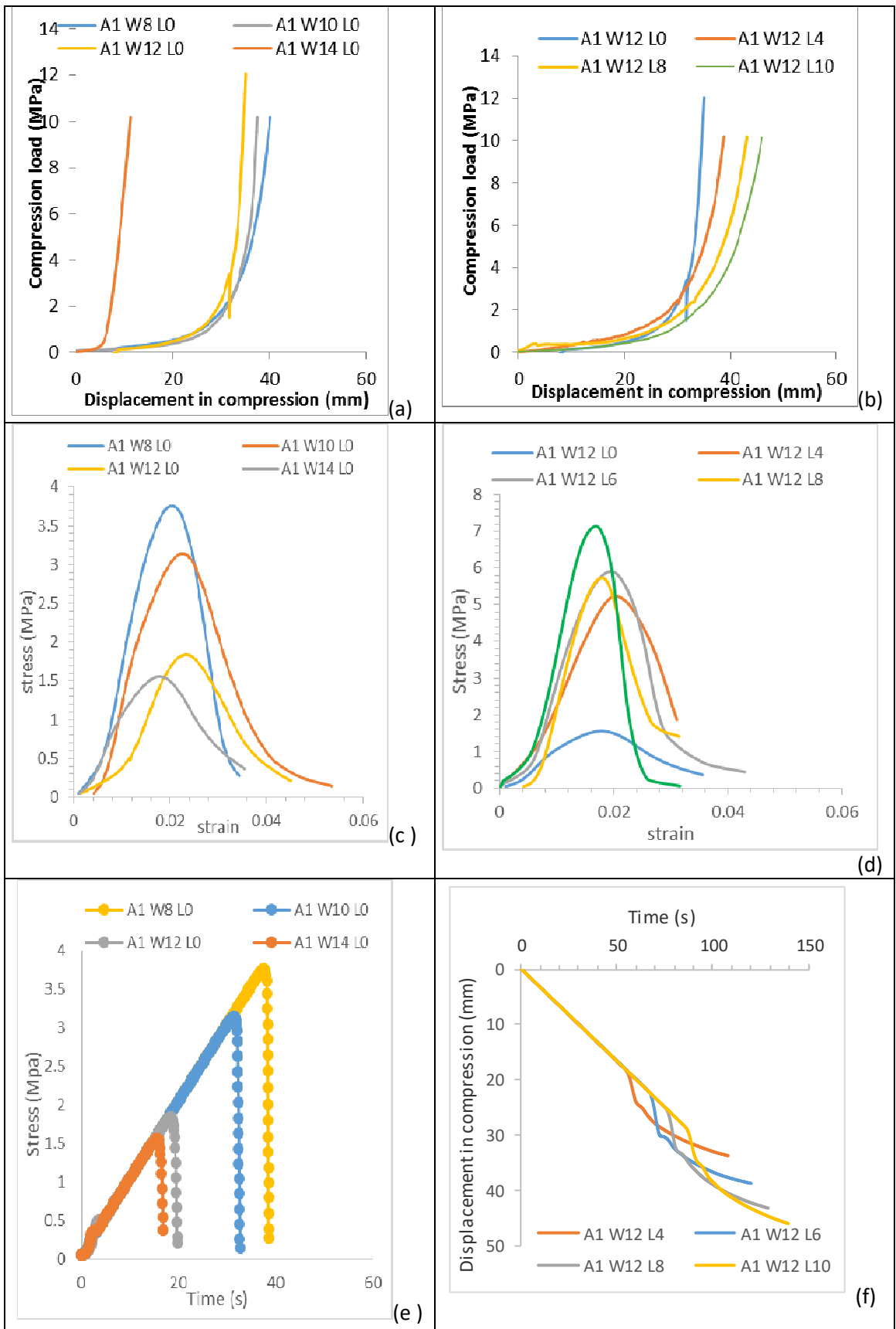
5

1 Fig. 9

2
3
4
5
6
7
8
9
10
11
12
13
14
15
16
17
18
19
20
21
22
23
24
25
26
27
28
29
30

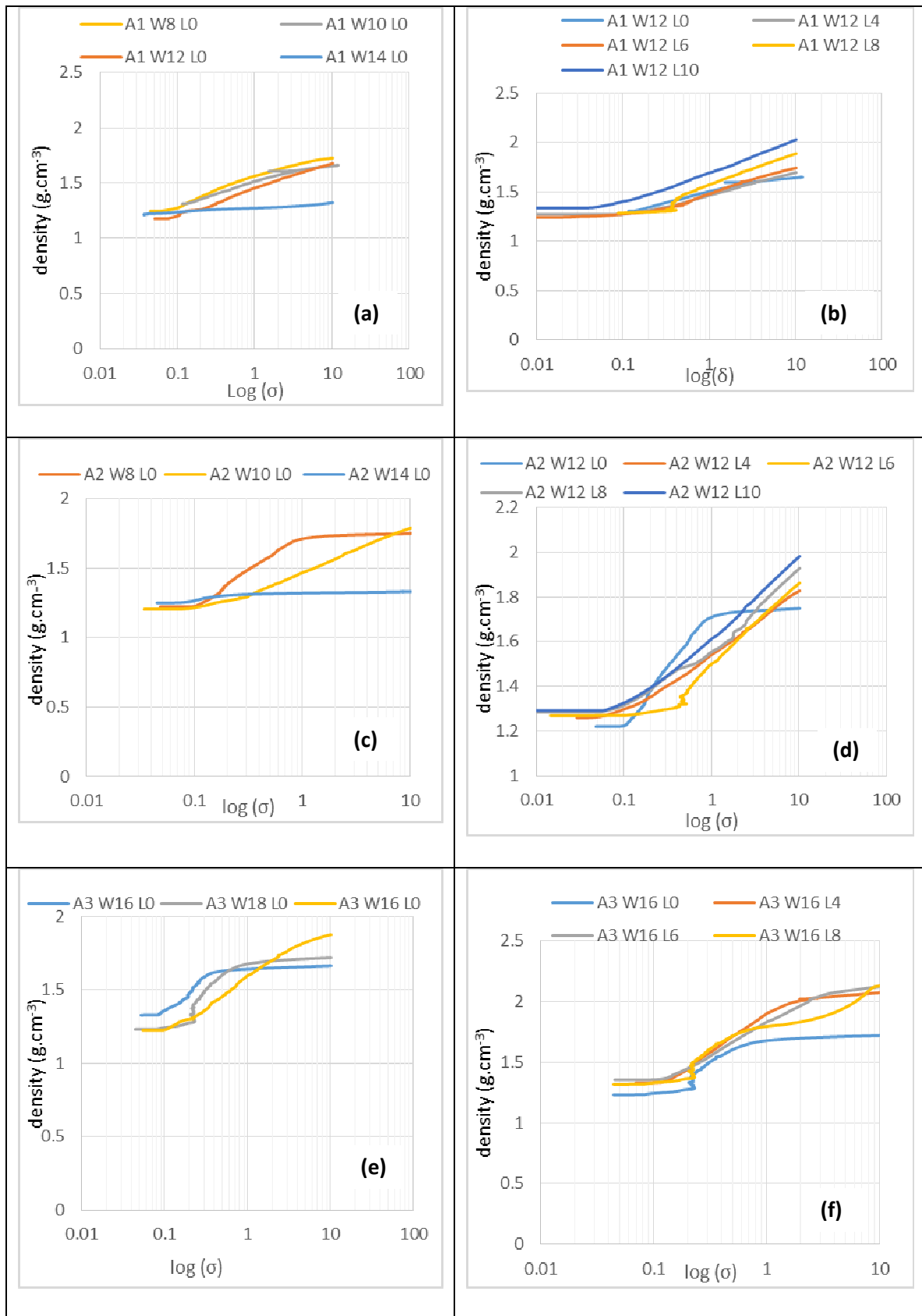


1 Fig. 10



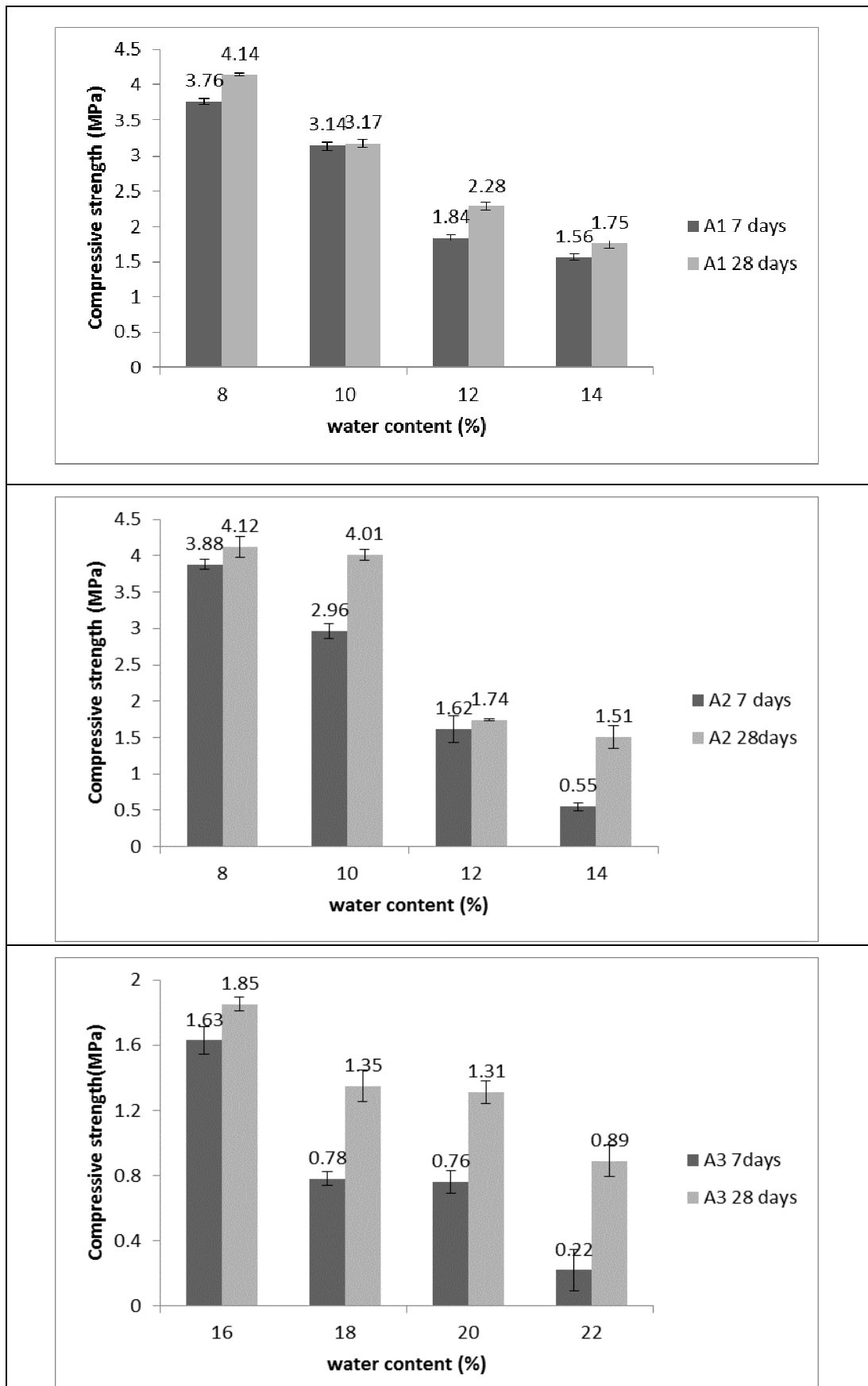
2

1 Fig. 11

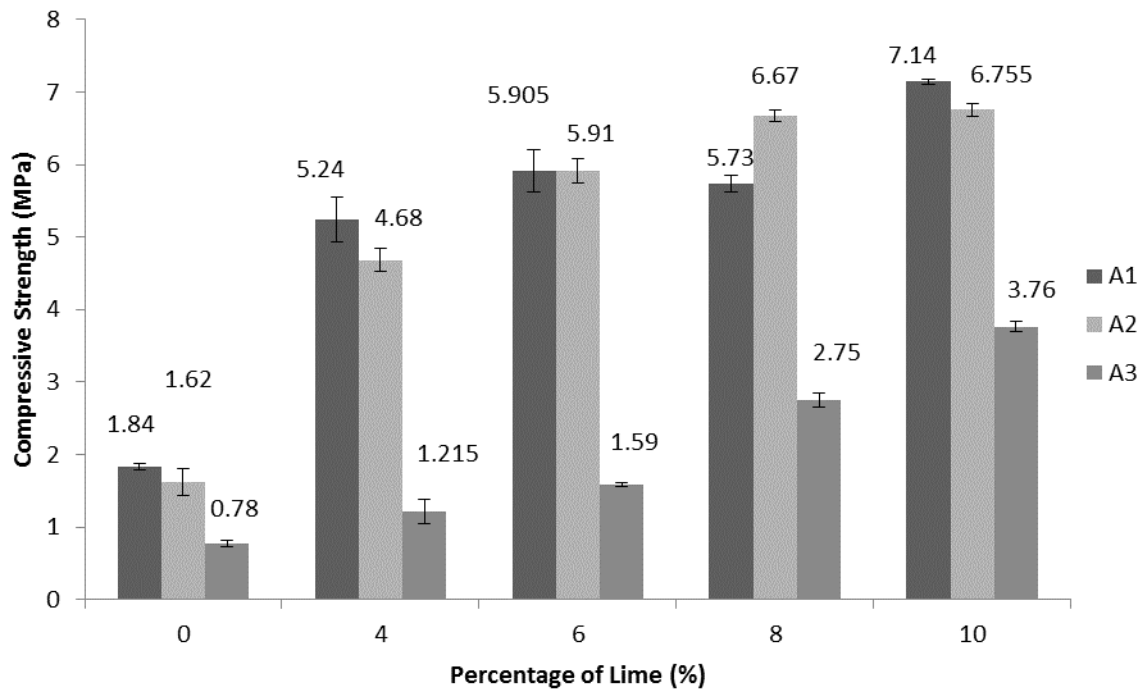


2

1 Fig. 12



1 Fig. 13



2
3
4
5
6
7
8
9
10
11
12
13
14
15
16
17
18

1
2
3
4
5
6
7
8
9
10
11
12
13
14
15
16
17
18
19
20
21
22
23
24
25
26
27
28
29
30
31

Table captions

- Tab.1 Grain size of collected clays
- Tab.2 Chemical analysis of studied clays (% by weight)
- Tab.3 Formulas used
- Tab.4 Values of Mass Loss for formulas studied
- Tab.5 Porosity and packing density values
- Tab. 6 Mixture composition effect

1
2
3
4
5
6
7
8
9
10
11
12
13
14
15
16
17
18
19
20

Table 1

samples	Clay (%)	Silt (%)	Sand (%)	d 10	d 30	d 60	C _u	C _c
A1	13.77	58.14	28.09	35.5	52.8	71.4	2.01	1.1
A2	19.62	46.48	33.9	41.1	53.6	65	1.58	1.08
A3	9.62	27.27	63.11	24.8	31.7	36.9	1.49	1.1
S	2.07	6.72	91.21	5.3	6.96	8.7	1.64	1.05

Table 2

Oxydes %	SiO ₂	Al ₂ O ₃	Fe ₂ O ₃	CaO	MgO	K ₂ O	Na ₂ O	TiO ₂	SO ₃	L.O.I	SiO ₂ /AL ₂ O ₃
A1	57.97	18.71	6	0.42	2.32	6.38	0.94	1	0.12	5.07	3.09
A2	57.33	20.97	5.15	0.14	1.99	3.73	0.54	1	0.16	6.42	2.7
A3	51.77	20.78	5.29	3.78	2.16	2.53	0.27	1	0.13	12.24	2.5

Table 3

Formulations	Clay type	% Sand	% Clay	% Lime
F 1	A 1	70	30	0
	A 2			
	A 3			
F 2	A 1	75	25	0
	A 2			
	A 3			
F 3	A 1	65	35	0
	A 2			
	A 3			
F 4	A 1	70	30	4
	A 2			
	A 3			
F 5	A 1	70	30	6
	A 2			
	A 3			
F 6	A 1	70	30	8
	A 2			
	A 3			
F 7	A 1	70	30	10
	A 2			
	A 3			

1 Table 4

Formulation	Loss mass (7 days)	Loss mass (28 days)	Drying shrinkage (%)
70S 30A1 8W	7.03	7.48	3.39
70S 30A1 10W	8.86	8.89	3.42
70S 30 A1 12W	8.94	9.18	3.75
70S 30A1 14W	9.71	9.79	3.9
70S 30A2 14W	8.9	8.97	4.2
70S 30A2 12W	8.79	8.91	3.8
70S 30A2 10W	8.69	8.74	3.56
70S 30A2 8W	8.66	8.69	3.38
70S 30A3 22W	13.36	13.39	4.68
70S 30A3 20W	13.33	13.36	4.24
70S 30A3 18W	13.26	13.28	4.13
70S 30A3 16W	12.02	12.12	4.11

2
3
4
5

a. Effect of water content and Setting time on samples studied

Formulation	Loss mass (%)	Drying shrinkage (%)
70S 30A1 12W 0L	8.94	3.75
70S 30A1 12W 4L	8.98	3.1
70S 30A1 12W6L	9.4	2.9
70S 30A1 12W 8L	9.9	2.36
70S 30A1 12W10L	10.9	2.33
70S 30A2 12W 0L	8.79	3.8
70S 30A2 12W4L	8.9	3.14
70S 30A2 12W 6L	9.6	2.82
70S 30A2 12W 8L	9.8	2.27
70S 30A2 12W 10L	10.1	2.11
70 S 30A3 18W 0L	13.26	4.11
70S 30A3 18W 4L	13.38	3.69
70S 30A3 18W 6L	13.5	3.49
70S 30A3 18W 8L	13.9	3.42
70S 30A3 18W 10L	13.93	3.16

6
7
8
9
10
11
12

b. Effect of lime added effect on samples studied

1 Table 5

2

3

Formulations	Porosity (%)	Packing density (%)
70S 30A1 8W	7.06	92.64
70S 30A1 10W	8.2	91.8
70S 30 A1 12W	8.3	91.7
70S 30A1 14W	8.86	91.14
70S 30A2 14W	8.62	91.38
70S 30A2 12W	8.60	91.4
70S 30A2 10W	7.88	92.12
70S 30A2 8W	7.86	92.14
70S 30A3 22W	17.12	82.88
70S 30A3 20W	15.73	84.27
70S 30A3 18W	12.94	87.06
70S 30A3 16W	10.93	89.07

11

a. Effect of water content effect on samples studied

12

Formulations	Porosity (%)	Packing density (%)
70S 30A1 10W	8.2	91.8
75S 25A1 10 W	8.67	91.30
65S 35A1 10W	8.33	91.67
70S 30A2 10W	7.88	92.12
75S 25A2 10W	9.67	90.03
65S 35A2 10W	9.58	90.42
70S 30A3 18W	12.94	87.06
75S 25A3 18W	14.05	85.95
65S 35A3 18W	14.57	85.43

13

b. Effect of mixture composition on samples studied

14

Formulations	Porosity (%)	Packing density (%)
70S 30A1 12W 0L	8.3	91.7
70S 30A1 12W 4L	7.81	92.19
70S 30A1 12W 6L	6.52	93.48
70S 30A1 12W 8L	6.33	93.67
70S 30A1 12W 10L	6.31	93.69
70S 30A2 12W 0L	8.60	91.4
70S 30A2 12W 4L	8.42	91.58
70S 30A2 12W 6L	7.85	92.15
70S 30A2 12W 8L	7.82	92.18
70S 30A2 12W 10L	7.32	92.68
70 S 30A3 18W 0L	12.94	87.06
70S 30A3 18W 4L	12.2	87.7
70S 30A3 18W6L	10.21	89.79
70S 30A3 18W 8L	9.17	90.83

15

c. Effect of lime added on samples studied

16

1 Table 6

2

Clay type	% Clay	% Sand	Compressive strength (MPa)
A 1	25	75	2.68
A 1	30	70	3.14
A1	35	65	2.87
A 2	25	75	0.59
A 2	30	70	2.96
A 2	35	65	1.19
A 3	25	75	0.69
A 3	30	70	0.78
A 3	35	65	0.68

3

4

5

6

7

8

9

10

11

12

13

14

15

16

17

18

19

20